Hybrid hydrogels with orthogonal transient crosslinking exhibiting highly tunable mechanical properties

Sofie Houben[1], Ana A. Aldana[2], An-Sofie Huysecom[3], Winy Mpinganzima[1], Ruth Cardinaels[3], Matthew B. Baker[2]*, Louis M. Pitet[1*]

[1]*Advanced Functional Polymers (AFP) Group, Institute for Materials Research (IMO), Hasselt University, Martelarenlaan 42, 3500 Hasselt, Belgium.*

[2]*Department of Complex Tissue Regeneration, MERLN Institute for Technology Inspired Regenerative Medicine, Maastricht University, P.O. Box 616, 6200 MD Maastricht, the Netherlands*

[3]*Soft Matter, Rheology and Technology, Department of Chemical Engineering, KU Leuven, 3000 Leuven, Belgium*

Abstract

Compositional changes in the chemical makeup of hydrogels offer a powerful strategy for fine-tuning of mechanical properties, enabling specific targeting for different applications. The chemical versatility exhibited by the tunable system introduced here can be leveraged to address a broad range of characteristics across the field of tissue engineering – from blood vessels to cartilage, for example, which demand materials with very different mechanical profiles. Furthermore, we rely exclusively on dynamic, non-covalent crosslinking to provide opportunities for 3D printing and injectability. This work describes a highly tunable system based on hydrogen bonding and ionic interactions. Single network hydrogels were made by exploiting various acrylic monomers including N-acryloyl glycinamide (NAGA) and acrylic acid (AAc). Additionally, hybrid hydrogels were explored by combining these acrylic networks with an ionically crosslinked alginate network. By combining orthogonal crosslinking strategies and altering the ratio between different components in these hybrid gels, a broad range of mechanical properties is demonstrated. The characteristics were extensively interrogated using tensile testing, compression testing, and rheological measurements. The final scaffolds were also shown to be biocompatible in preliminary cell-viability studies.

Introduction

The ever-increasing attention given to hydrogels as biomaterials has steered the structural design into various innovative directions. Hydrogels are crosslinked polymer networks containing large amounts of water (ca. 70–95 wt %). They have great potential to be biocompatible due to their structural similarity to the extracellular matrix (ECM). Their high water content and chemical versatility have spurred enormous interest in medical applications like tissue engineering and wound dressings.[1-5] However, the large span of potential applications requires accessibility to an equally broad range of mechanical properties, which are often difficult to obtain with compositionally simplistic formulations and conventional molecular architectures. Especially for load-bearing tissues, such as cartilage in the meniscus, obtaining the desired mechanical properties remains a challenge. Several design strategies have been developed to overcome these mechanical limitations.[6] Double network hydrogels emerged as a strategy to toughen gels by combining two polymer networks with contrasting crosslinking densities. [7] Throughout the years DN hydrogels gained attention as biomaterials as a result of the wide variety of mechanical properties obtainable, and many of these DN hydrogels have been tested for their compatibility with modern additive manufacturing technologies.[8]

Looking toward non-invasive implantation and customizable scaffold constructs, these materials should ideally be able to be injected.[8-13] Conventional hydrogels are typically covalently crosslinked. The permanent nature of covalent linkages renders these materials unsuitable for processing techniques like injection and 3D printing. On the contrary, dynamic crosslinking strategies such as hydrogen bonding and ionic interactions offer the possibility for shear-thinning behavior or self-healing properties, which are critical aspects for injectability or printability. The majority of hydrogels adopt covalent, irreversible crosslinking for at least one of the networks, while only a small amount of these hydrogels utilize exclusively dynamic reversible crosslinking strategies, highlighting the need for tough, fully dynamic hydrogels.[8]

N-acryloyl glycinamide (NAGA), first reported in 1964, is an appealing building block in this regard.[14] NAGA's dual amide structure enables interchain hydrogen bonding between poly(N-acryloyl glycinamide) (PNAGA) repeating units, rendering hydrogels from this polymer remarkably tough.[15, 16] The nature of the dynamic hydrogen bonding also renders these hydrogels thermoresponsive, with the

position of the sol-gel transition (i.e., upper-critical solution temperature – UCST) depending on the concentration and molar mass.[17] Combining NAGA with different acrylate monomers such as acrylic acid, acrylamide, and N-isopropylacrylamide (NiPAAm) leads to copolymers exhibiting a broad range of sol-gel transition temperatures, and thus offers a convenient handle for fine-tuning the properties.[17-21] This tunable sol-gel transition renders PNAGA gels injectable under various conditions [22, 23] and also applicable in 3D printing.[21, 24, 25] Owing to the adaptability and structural variations attainable, PNAGA hydrogels have garnered significant attention for applications in drug delivery[26], wound healing [27], strain sensors [28], and tissue engineering.[22-25, 29-33]

This work demonstrates a significant extension of PNAGA as a versatile building block, wherein we demonstrate a highly tunable system exhibiting an impressive array of mechanical properties. The remarkable tunability is achieved by variation of the composition and crosslinking in hybrid hydrogels comprised of two complementary networks with fully dynamic, orthogonal crosslinking. Herein, the term hybrid hydrogel refers to materials with two networks from distinctly different origins. In this case we have synthetically derived acrylic networks combined with biologically derived alginate networks. First, individual single network (SN) hydrogels were prepared, in which both hydrogen bonding and ionic crosslinking have been leveraged to different degrees. These SN hydrogels comprised acrylic based networks, which were obtained from combination/copolymerization of the monomers N-acryloyl glycinamide (NAGA) and acrylic acid (AAc). These networks were subsequently combined with a second network, ionically crosslinked alginate, to obtain hybrid hydrogels. Variations in the alginate network were made by exploring different ions responsible for crosslinking the alginate chains (Ca^{2+} and Fe^{3+}). The hybrid materials are conceptually illustrated in Figure 1, accompanied by the respective polymer structures and orthogonal crosslinkers that are possible between the various constituents. P(NAGA-co-acrylic acid) can be crosslinked by hydrogen bonding as well as ionic crosslinking (Figure 1C). It can be combined with alginate, a biopolymer with ionizable carboxyl groups that can be leveraged in ionic crosslinking (Figure 1A), to form interpenetrating network hydrogels (Figure 1B). Polymer structures containing acrylic acid repeating units can also participate in ionic crosslinking with the alginate, which is an important aspect that establishes the final material properties (Figure 1E) (*vide infra*). Our strategy represents a versatile and easily adaptable approach to finely tune the mechanics of

a complex hydrogel construct, while maintaining a fully dynamic system that is potentially primed for contemporary delivery and implantation methods, like injection. The results demonstrate a remarkably broad range of mechanical properties that are accessible through straightforward adjustments to the recipe. The final constructs are also easily functionalizable for further tailoring *in vivo* interactions.

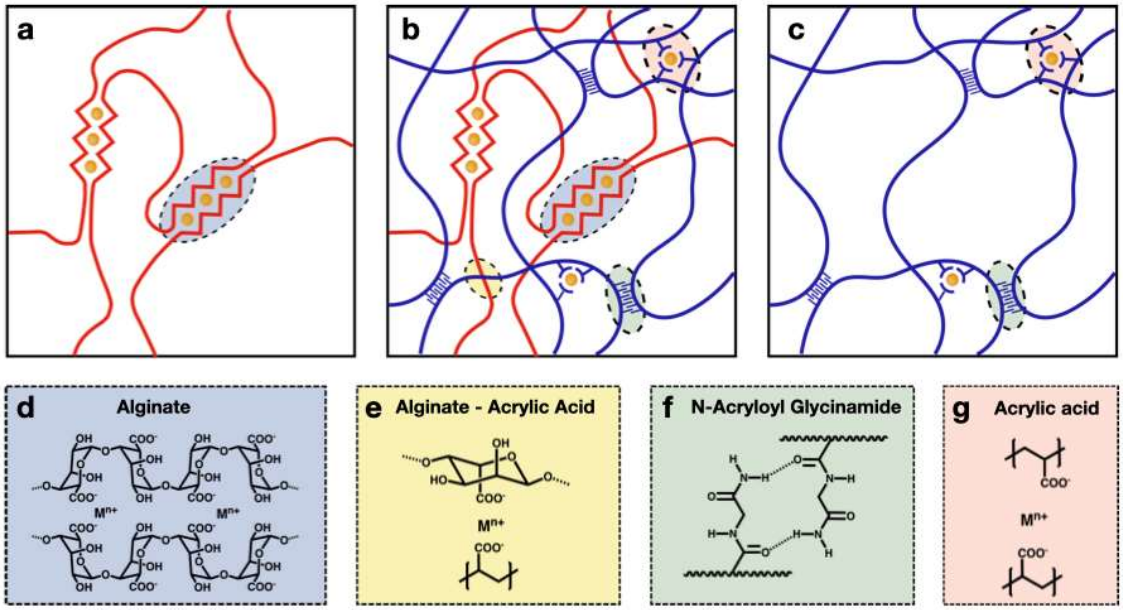

Figure 1: *A) Alginate single network hydrogel ionically crosslinked by multivalent cations (M^{n+} = Ca^{2+} or Fe^{3+}). B) Alginate/Poly(N-acryloyl glycinamide-co-acrylic acid) hybrid hydrogel crosslinked by ionic interactions between alginate chains and between alginate and acrylic acid and hydrogen bonds between PNAGA. C) P(NAGA-co-Acrylic Acid) single network hydrogel crosslinked by hydrogen bonding and ionic interactions. D) ionic crosslinking of alginate by multivalent cations (M^{n+} = Ca^{2+} or Fe^{3+}). E) Ionic crosslinking in the hybrid hydrogel between alginate and acrylic acid. F) Hydrogen bonding between NAGA units. G) Ionic crosslinking between acrylic acid units.*

Results and Discussion

All gels presented in this work are coded as XX-W-a/b/c/M, where W is the weight fraction of water; a, b, and c are the weight fractions of NAGA, AAc, and alginate, respectively; XX represents the type of hydrogel (SN for single network hydrogels or IPN for interpenetrating network hydrogels); M represents the metal ion used for ionic crosslinking (Fe for iron(III), Ca for calcium (II)).

Single network hydrogels.

Single network PNAGA hydrogels were made in a one-step/single-pot method using lithium phenyl-2,4,6-trimethylbenzoylphosphinate (LAP) as a biocompatible photoinitiator. NAGA was synthesized according to a previously reported synthesis method (Figure S2, S3, S4). NAGA and LAP (0.4 mol % relative to NAGA monomer) were dissolved in water, the solution was poured into molds and cured for 30 minutes under UV light (254 nm) at ambient temperature (see Supporting Information for details on molds and experimental procedure, Figure S1). A series of NAGA-based hydrogels was explored, and the mechanical properties were compared by tensile tests (Figure 2; Table S1). SN PNAGA gels form shape-retaining, transparent, colorless gels that show increased strength and elastic modulus with decreasing initial water content (i.e., increasing polymer content), presumably due to a higher number of entanglements per chain.[34] At higher polymer content (e.g., 30 wt % NAGA), these fully dynamic hydrogels exhibit remarkable mechanical properties in tensile tests (fracture stress = 1.1 MPa, fracture strain = 500% and Young's modulus, E = 400 kPa). Single network PNAGA hydrogels routinely expel water after curing due to rearrangements of the hydrogen bonds. Therefore, the gels are soaked in water after curing until the equilibrium water content (EWC) is reached. True water percentages were measured 24 hours after this soaking step. Depending on the initial weight percentage of NAGA in the gel-precursor solution, different equilibrium water contents were obtained in the final hydrogel constructs (see Table S2, Figure S5).

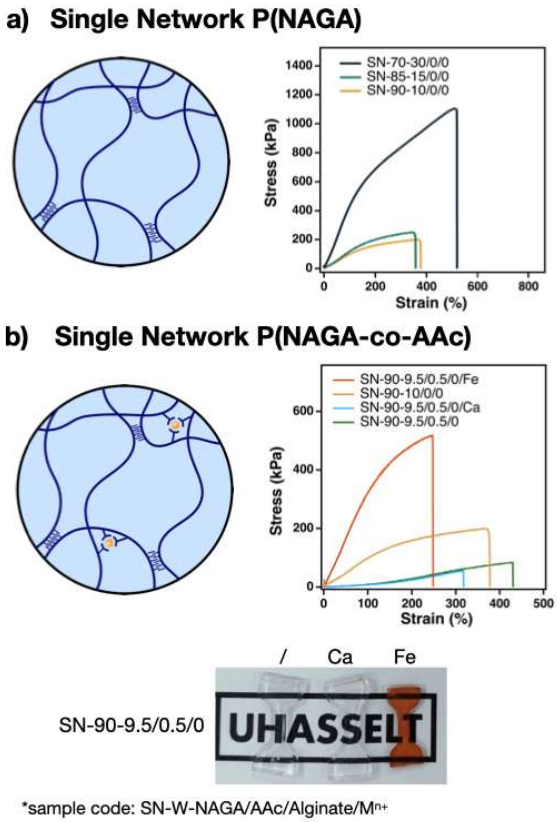

Figure 2: *A) Comparison of stress-strain curves of single network PNAGA hydrogels. Higher polymer concentration leads to tougher materials due to higher degree of entanglements. B) Comparison of PNAGA and P(NAGA-co-AAc) hydrogels. Addition of 0.5 wt% AAc to the polymer backbone (green/blue) reduces the toughness of the resulting hydrogel compared to a PNAGA homopolymer hydrogel (yellow) when no ions or Ca^{2+} ions are present. Increase in toughness is only obtained when addition of 0.5 wt% AAc is combined with addition of Fe^{3+} ions (red).*

Our strategy at this stage was to broaden the array of accessible properties by introducing complementary components into the original formulations. Hydrogels containing copolymers of NAGA with acrylic acid were synthesized in an analogous manner to test the effect of hydrogen bonding. AAc has routinely been used as a component in tough hydrogels, owing to its ability to form strong yet dynamic hydrogen bonds and ionic bonds with certain multi-valent counterions.[35, 36] However, to date, its combination with NAGA remains unexplored. Acrylic acid contains a *single* carboxylate group and subsequently forms hydrogen bonds that are significantly weaker compared to NAGA's dual hydrogen bonds. Copolymerizing NAGA with acrylic acid (figure 2B, green) effectively lowers the concentration of hydrogen bonds for a given polymer concentration and therefore results in significantly lower Young's modulus and toughness compared to homopolymer PNAGA gels (Figure 2B, yellow). We

observed the same effect when diluting the NAGA with an alternative monomer, acrylamide (AAm) to form SN copolymers with various concentrations. The stiffness decreases monotonically with decreasing NAGA content, irrespective of the comonomer structure, pointing consistently toward the hydrogen-bonding as the primary factor contributing toward strength/stiffness in SN gels (Figure S8). However, the AAc comonomer was strategically explored for ionic crosslinking, which fortifies the structural integrity as an orthogonal dynamic linkage. Ionic crosslinking occurs in PAAc as a virtue of a multi-valent counter-ion (e.g., Fe^{3+}) complexing with the carboxylate repeating units on the polymer backbone, provided the pH is high enough to deprotonate the acids. In this work, iron (III) or calcium (II) ions were introduced by soaking the pre-formed hydrogels in a 0.1M $FeCl_3$ or 0.1M $CaCl_2$ aqueous solution. P(NAGA-co-AAc) hydrogels crosslinked by calcium ions are colorless transparent gels, while those crosslinked by iron (III) ions are orange transparent gels (Figure 2B). Adding calcium (Ca^{2+}) ions as a crosslinking agent to P(NAGA-co-AAc) hydrogels doesn't improve the mechanical properties compared to the same gels without any additional crosslinking added (Figure 2B). On the contrary, the addition of the ferric ions leads to a higher crosslinking density compared with the non-complexed copolymer and thus results in an increased elastic modulus and a higher fracture strength. The contrast between the calcium and iron crosslinked P(NAGA-co-AAc) hydrogels can be explained by the difference in coordination with acrylic acid's carboxyl groups. Divalent cations interact with two carboxyl groups leading to a lower coordination number ($(COO^-)_2Ca^{2+}$) compared to trivalent cations that interact with three carboxylic acid groups ($(COO^-)_3Fe^{3+}$). The higher coordination number of iron leads to a more compact network and a denser crosslinking structure resulting in a significant increase in the toughness of the resulting gels. Substituting just 0.5 wt% of NAGA with iron crosslinked acrylic acid increases the Youngs modulus from 74 kPa for SN PNAGA hydrogels (SN-90-10/0/0) to 276 kPa for SN P(NAGA-co-AAc) hydrogels (SN-90-9.5/0.5/0/Fe) (Table S2, Table S4 & Figure S7).

Like single network PNAGA gels, the higher crosslinking density causes the gels to expel some of the water from the initial formulation, leading ultimately to lower water content in the final construct. Exploiting AAc comonomers demonstrates the tunability of gels that are fortified by dynamic hydrogen bonding. Varying copolymer composition, crosslinking density, and water content all have a dramatic influence on the mechanical properties, providing multiple independent handles to fine-tune the

mechanical response. All these single network materials are toughened because of the combination of dynamic crosslinking and the extensive entanglements of the polymer chains. We surmise that the threshold for transitioning to a highly entangled initial polymer network occurs between the initial water concentrations of 70% and 85%, as evidenced by the dramatic increase in tensile strength and toughness. This is consistent with the observations made by Suo and co-workers in comparing gels made from initially concentrated precursors versus dilute networks.[34]

Interpenetrating network hydrogels

Combining two independent polymer networks with contrasting mechanical properties is an appealing strategy for obtaining toughened hydrogel materials.[7] Combining alginate as an additional network with PNAGA offers an orthogonal second type of crosslinking. Alginate is routinely crosslinked ionically by multivalent cations such as Ca^{2+} or Fe^{3+}.[37] We surmised that this adds an additional dimension for expanding both the range of mechanical properties as well as potentially improving functionality and biocompatibility. Interpenetrating network (IPN) hydrogels were made using a procedure similar to the one for single network hydrogels. NAGA, LAP, and alginate were dissolved in water, and the solution was poured into molds and cured for 30 minutes under UV light (254 nm) at ambient temperature (see Supporting Information for details on molds and experimental procedure, Figure S1). Ionic crosslinkers are introduced after curing by soaking the resulting gels in an ionic solution ($CaCl_2$ or $FeCl_3$, 0,1M).

As reported in literature, different cations have different effects on the mechanical properties of the resulting gels owing principally to the different ionic strength and valency.[37] Counterintuitively, tensile strength, elastic modulus, and elongation at fracture all deteriorate when ionically crosslinked (both Ca^{2+} and Fe^{3+}) alginate is included as a second network with PNAGA gels (Figure 3) at a given solids concentration in comparison with the SN gels. This can be attributed to the dilution of the hydrogen bonding compared with pure PNAGA gels and the combination of two highly crosslinked dynamic networks. Special care was taken to keep the initial water content constant while making the IPN hydrogels with PNAGA and alginate. Therefore, we compensate for any alginate that is added to the IPNs by removing a commensurate amount of NAGA, leading intrinsically to a lower degree of

hydrogen bonding compared to the SN hydrogels. Similar to the SN copolymer hydrogels, diluting the hydrogen bonds by adding an orthogonal network led to a decrease in elastic modulus and tensile strength (Table S6, Figure S9).

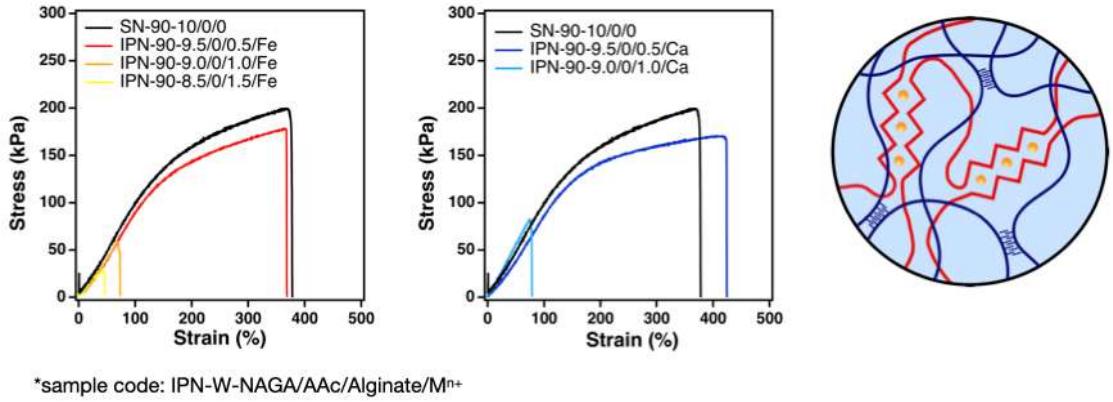

Figure 3: IPN PNAGA/M-Alginate hydrogels. *Tensile stress-strain curves for PNAGA/M^{n+}-alginate double network hydrogels crosslinked by Ca^{2+} or Fe^{3+}. The PNAGA network is crosslinked by hydrogen bonds while the alginate network is ionically crosslinked by Ca^{2+} or Fe^{3+} ions.*

This combination runs counter to the well-established concept of toughened dual network gels, in which two networks with highly contrasting crosslink densities must be employed.[38] The AAm/alginate double network hydrogels reported by J. Y. Sun et. al., for example, show an increasing modulus with increasing alginate content and a toughness that reaches a maximum in hybrid gels.[39] In PAAm/Alginate hydrogels, the ionically crosslinked alginate network provides an energy dissipation mechanism, while the covalently crosslinked acrylamide network with its long chains provides extensibility while keeping the hydrogel in shape. This is not the case for the PNAGA/Alginate hydrogels, as the H-bond crosslinked NAGA network is too densely crosslinked to enable significant extensibility. With pure PNAGA gels already being quite tough, addition of alginate does not provide any improvements, particularly in modulus. We emphasize here, however, that the more conventional PAAm-alginate hybrids contain covalently crosslinked PAAm networks, and therefore offer no possibilities for recovery after destructive extension, while PNAGA/alginate hydrogels are fully dynamically crosslinked.

Notably, the single network PNAGA gels perform remarkably well, despite having no permanent crosslinking. To exclude the possibility of ions such as Ca^{2+} or Fe^{3+} influencing hydrogen bonding, single network PNAGA hydrogels were exposed to these ions (i.e., $CaCl_2$ or $FeCl_3$). However, this revealed marginal influence on the mechanical properties (Figure S6). The actual ion concentrations

were not quantified in these experiments, but visually the Fe^{+3} samples became dark orange in color, suggesting a significant ion uptake. While there seems to be little mechanical benefit of adding alginate to the system, it potentially provides opportunities for additional functionality, as it adds the possibility of improving cell viability by biofunctionalizing the alginate with, for example, RGD peptides, or increasing the viscosity for 3D printing applications.[40-42]

We set out to enhance the mechanical properties of the functionally versatile hybrid gels by exploiting once again the AAc comonomer in the network. AAc monomer was used strategically to fortify the mechanical integrity of the hybrid hydrogel scaffolds, whereby extraordinarily tough IPN hydrogels were realized, similarly to the toughened single network PNAGA hydrogels. Both Ca^{2+} and Fe^{3+} were introduced for ionic crosslinking in the IPN P(NAGA-co-AAc)/M-alginate hydrogels, with those crosslinked by calcium being colorless transparent gels and those crosslinked by iron being orange transparent gels (Figure 4A).

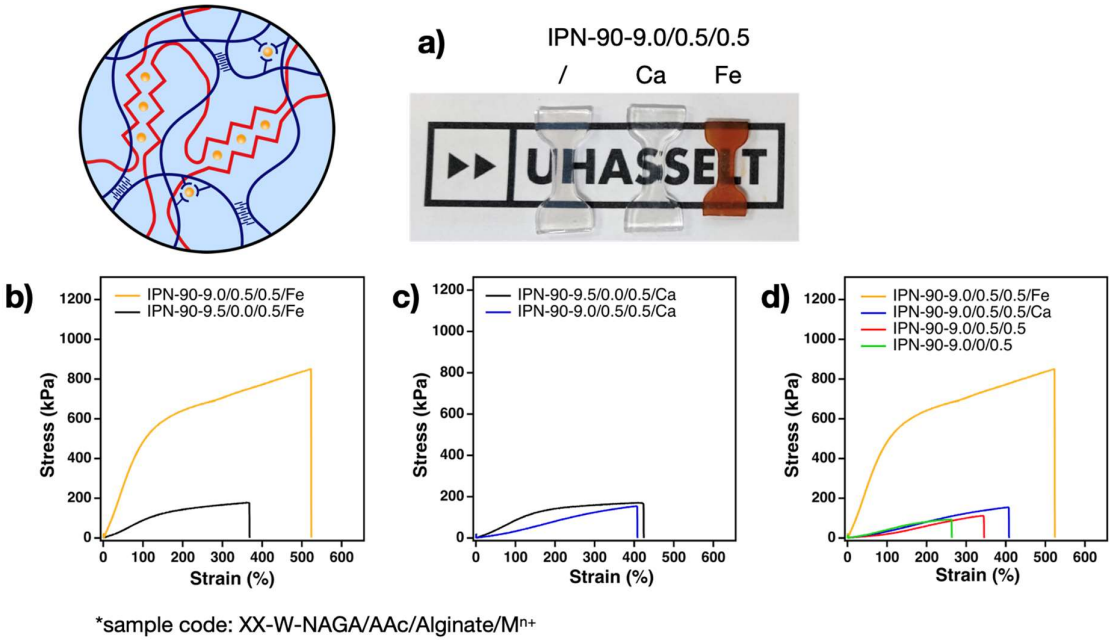

Figure 4: IPN P(NAGA-co-AAc)/M-Alginate hydrogels *a) Visual of P(NAGA-co-AAc)/M-Alginate hydrogels crosslinked by calcium(II) or iron (II). b) Comparison of stress-strain curves of IPN PNAGA/Fe-Alginate (black) and IPN P(NAGA-co-AAc)/Fe-Alginate (Yellow). c) Comparison of stress-strain curves of IPN PNAGA/Ca-Alginate (black) and IPN P(NAGA-co-AAc)/Ca-Alginate (Blue). d) Comparison of stress-strain curves of IPN P(NAGA-co-AAc)/Ca-Alginate without ionic crosslinker (red), crosslinked by iron(III) (yellow) or calcium (II) (blue) as well as IPN P(NAGA)/Alginate (green).*

Similar to the single network hydrogels, introducing 0.5wt% of acrylic acid into the PNAGA backbone is detrimental to the mechanical properties of the resulting IPN P(NAGA-co-AAc)/Alginate (IPN-90-9.0/0.5/0.5) hydrogel compared to the IPN PNAGA/Alginate (IPN-90-9.5/0.0/0.5) hydrogel when no additional ionic crosslinking is added (Figure 4D). This effect is due to further dilution of the hydrogen bonding and is in line with the observations in single network hydrogels. Upon addition of Fe^{3+} ionic crosslinker, the tensile strength and modulus greatly improve compared to PNAGA/Alginate, despite only 0.5 wt % of acrylic acid being incorporated (Figure 4B) while Ca^{2+} leads to a decrease in tensile strength and modulus (Figure 4C).

Interestingly, in the case of P(NAGA-co-AAc) copolymers crosslinked by iron and calcium, adding alginate to the hydrogel does improve the mechanical properties (Figure 5A&B). Adding just 0.5 wt% of alginate to a P(NAGA-co-AAc) hydrogel leads to an increase in Young's modulus from 276 kPa for SN P(NAGA-co-AAc) (SN-90-9.5/0.5/0/Fe) to 552 kPa for IPN P(NAGA-co-AAc)/Alginate (IPN-90-9.0/0.5/0.5/Fe) when crosslinked with iron (Table S4 & Table S10). This illustrates the importance of the connection formed between the acrylate network and the alginate network through the ionic interaction between acrylic acid residues and carboxylic acid groups of alginate (Figure 1E). Further improvement in the mechanical properties can be obtained when the polymer concentration is increased. When the water content of the gels is decreased from 90% water to 70% water while keeping the ratio of the components the same, an increase in Young's modulus from 552 kPa (IPN-90-9.0/0.5/0.5/Fe) to 1.5 MPa (IPN-70-27/1.5/1.5/Fe) is observed (Figure 5C, Table S10). The increase in tensile strength and stiffness comes at the expense of slightly lower extensibility. This, however, is less relevant when looking at applications like cartilage tissue engineering, where increased stiffness is a key feature. Even when looking at ligaments or tendons which have an ultimate strain of 20 to 40%, the copolymer hydrogels still have excess extensibility.[43]

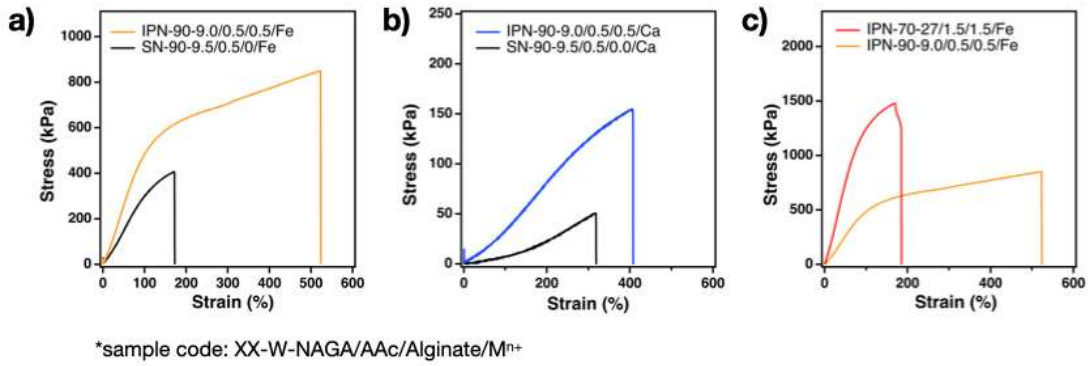

Figure 5: *A) Comparison of stress-strain curves of IPN P(NAGA-co-AAc)/Fe-Alginate (Yellow) with iron (III) crosslinked SN P(NAGA-co-AAc) (black). B) Comparison of stress-strain curves of IPN P(NAGA-co-AAc)/Ca-Alginate (Blue) with calcium crosslinked SN P(NAGA-co-AAc) (black). C) Comparison of stress-strain curves of IPN P(NAGA-co-AAc)/Fe-Alginate made at 90% (yellow) or 70% (red) water.*

Looking at applications that require mechanical properties that mimic load-bearing tissues, compressive properties are critical. Therefore, SN PNAGA and IPN P(NAGA-co-AAc)/Alginate gels were tested for their compressive properties and swelling behavior (Figure 6). Gels were typically swollen for 24 h, after which we surmised that equilibrium had been reached. Swelling for significantly longer did not result in appreciable changes. In compression testing, the addition of ionically crosslinked acrylic acid also leads to a remarkable increase in compression modulus from 33 kPa for SN PNAGA to 383 kPa for IPN P(NAGA-co-AAc)/Fe-Alginate at 90% water (Figure 6a, Table S11). Lowering the water content of the hydrogels to 70% enables even more pronounced enhancement of mechanical response. We observed an increase in compressive modulus from 383 kPa (IPN-90-9.0/0.5/0.5/Fe) to 1.6 MPa (IPN-70-27/1.5/1.5/Fe) (Figure 6a; Table S11). Compressive moduli of native cartilage fall between 1 to 20 MPa, depending on the position in the body. [44, 45] While the moduli of the high-water content hybrid hydrogel fall short of the target, the hydrogels at 70% water reach the lower end of this range. In fact, water content in native cartilage is closer to 70% water. Further modulation is also possible with the various component handles built into this versatile hybrid system.

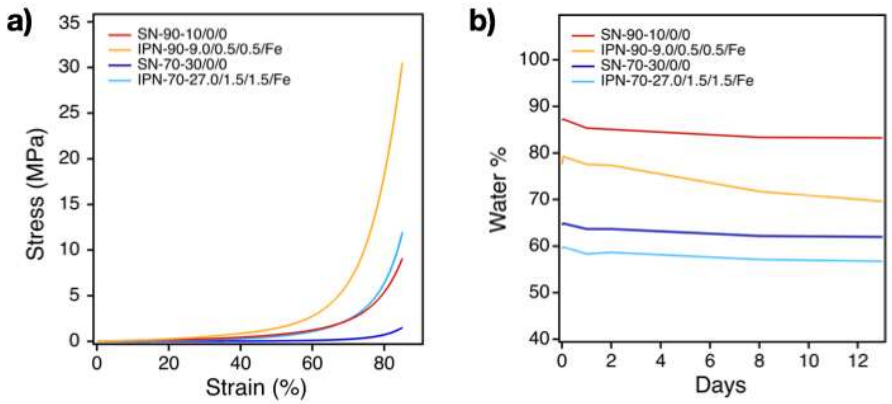

Figure 6: *A) Compression stress-strain curves for SN PNAGA and IPN P(NAGA-co-AAc)/Fe Alginate hydrogels made at 90% and 70% water. B) Evolution of water content during swelling experiments measured gravimetrically for SN PNAGA and IPN P(NAGA-co-AAc)/Fe Alginate hydrogels made at 90% and 70% water.*

Turning towards oscillatory rheology, we were interested in investigating any dynamic character of these hydrogels, due to their non-covalent crosslinking mechanisms. Time sweeps, strain sweeps, and frequency sweeps were measured for SN PNAGA, IPN P(NAGA)/Fe-Alginate, and IPN P(NAGA-co-AAc)/Fe-Alginate gels (Figure S12 & S13), and the resulting trends in moduli comply with those from tensile and compression testing (Table S12). Hydrogels that show an increase in Young's modulus also have higher shear dynamic moduli G' and G" in time, frequency, and strain sweeps, while a lower linear stress–strain limit (extensibility) in tensile tests is met with a lower linear strain limit in rheological strain sweep experiments.

In the frequency sweeps, we do not observe a crossover point at the time scales investigated; however, we do see significant changes in the loss modulus over time for the more dynamic Fe hydrogels, indicating temporal changes in the crosslinking as characteristic of dynamic hydrogels. The single network hydrogels show extremely slow convergence at lower frequencies, also indicating that these systems have extremely slow internal network dynamics. Performing a multimode Maxwell analysis of the limited curves also shows this trend. The single network and IPN Ca hydrogels all have a longer final (120 s) relaxation mode, that is the major contributor to the network; the IPN Fe hydrogels have a faster final relaxation mode (60 s), again the major contributor to the network. While the limited window of the frequency sweep has difficulty capturing longer timescale relaxations, we already begin

to see differences in the internal dynamics of the hydrogels tested. The plateau modulus, as determined for each mode using the multimode maxwell model, was converted to the number density of elastically active chains using the affine network theory. The total amount of elastically active chains increases when additional components are added to the system, which can be related to an increasing number (density) of crosslinks in the system, which translates ultimately to a higher modulus (Table S13). Similar to the increase in modulus observed through compression testing, the addition of alginate leads to an increase in the total amount of elastically active chains. An even more drastic increase is seen upon the addition of ionically crosslinked acrylic acid together with a clearly different G" behavior at low frequency.

One downside of using P(NAGA-co-AAc) copolymer is that the higher degree of crosslinking leads to the gels expelling water over time, even when submerged in water. The copolymer gels made at 90% initial water content go down to 70% water after being submerged for 14 days while the gels made at 70% initial water content go down to 60% (Figure 5b; Table S11). However, this is still in the range of biological tissues such as ligaments and tendons (60% water), epithelial tissue (65% water) or cartilage (75% water).[46] The equilibrium water content (EWC) should be taken into consideration when designing the system and targeting final mechanical responses. The trends in EWC, however, are consistent across the range of formulations investigated in this work.

The cytotoxicity of biomaterials for tissue engineering applications is a critical consideration, ultimately aiming toward constructs that are suitable as *in vivo* implantations. Fibroblasts, predominantly present in connective tissues, are commonly used for testing new biomaterials because they take an active part in the immune response, inflammatory processes and wound healing.[47, 48] We evaluated the cell viability of human dermal fibroblasts (HDFs) on 3 key hydrogel formulations, SN PNAGA, hybrid PNAGA/Alginate and hybrid P(NAGA-co-AAc)/Alginate, to evaluate the effect of each additional component. After 24 hours, HDFs cultured on all NAGA-based hydrogels (90% water) showed high viability (most of the cells are stained in green, see Figure 6). Due to the lack of adhesive sites (e.g. RGD peptide sequence) in all hydrogels, most of cells grew in the bottom of the wells. The majority of cells cultured on NAGA-based hydrogels without AAc were alive at day 4, while very low cell viability was found on hydrogels with AAc. Probably, the high swelling observed in both AAc-

based hydrogels does not allow cells for taking nutrients from culture media. On the other hand, HDFs were also cultured on the IPN-70-27/1.5/1.5/Fe hydrogel. However, live cells were not observed on that hydrogel (Figure S11). Probably, the high concentration of iron ions released to culture media affects the cell viability. The great amount of live cells on both single network PNAGA gels (at 90 and 70% water) and IPN PNAGA/Ca-Alginate hydrogels indicates that these formulations are cytocompatible with human dermal fibroblasts, and thus potentially promising for tissue engineering applications. Clearly, caution must be used with iron in biomedical applications. Ionic crosslinking in general comes with concerns about ion leaching, and alternative crosslinking strategies (e.g., dynamic covalent bonding) should be evaluated as possible alternatives.

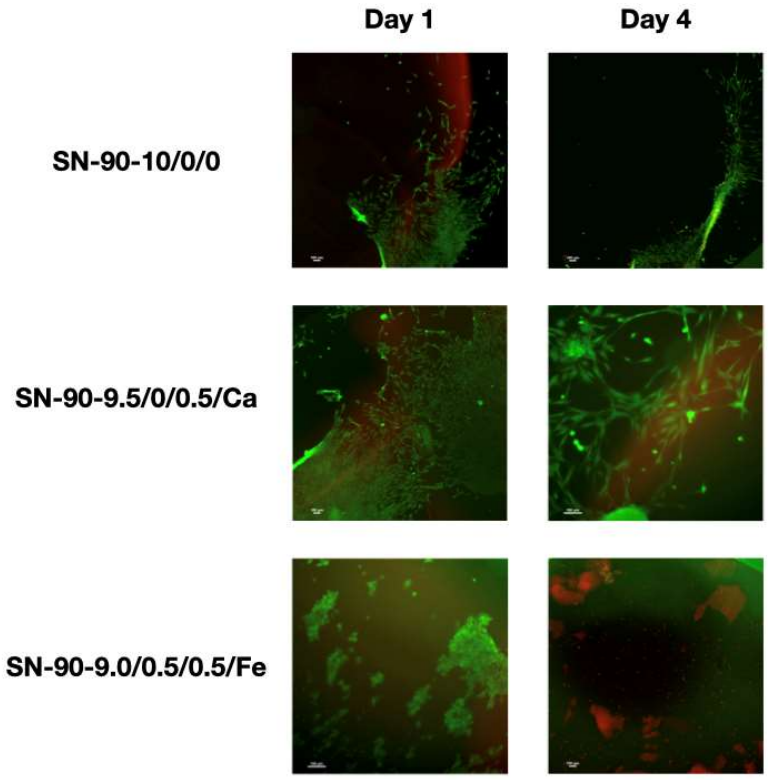

Figure 6. *10% PNAGA, 9.5%PNAGA/ 0.5% Ca-Alginate and 9.0% PNAGA/0.5% Ca-Alginate/0.5% AAc hydrogels are cytocompatible for human dermal fibroblasts. Images of HDF cells stained with calcein-AM (green, live) or ethidium homodimer (red, dead) after 1 and 4 days on the single network and interpenetrating network hydrogels. Scale bar: 100 μm.*

Conclusion

We successfully created single network hydrogels consisting of exclusively dynamic cross-linking. By tuning the ratio of monomers N-acryloyl glycinamide and acrylic acid, the strength of the gels can be varied. The dual hydrogen bonding between NAGA units along the polymer backbone already provides the hydrogels with high stability and strength. When copolymerized with acrylic acid, the gels weaken because of the dilution of the hydrogen bonding. However, the strength of SN PNAGA gels was improved by incorporating a small amount of ionically crosslinked acrylic acid, leading to a drastic increase in elastic modulus and strength. This concept was extended to hybrid hydrogels in which copolymers of the previously mentioned monomers are combined with ionically crosslinked alginate. Similar trends were observed for the hybrid gels, with the dilution of the hydrogen bonding leading to weaker gels. Acrylic acid was used again in combination with iron (III) ions to strengthen the constructs. In this work, we demonstrated a highly tunable system with mechanical properties in the range of those of cartilage. While alginate provides little to no added value in terms of mechanical strength, it provides the possibility of improving cell viability or increasing the viscosity for 3D printing applications.

ASSOCIATED CONTENT

Supporting Information

The supporting information is available free of charge at https://

Materials and methods, additional supporting experimental details including stress–strain plots.

AUTHOR INFORMATION

Orcid:

Sofie Houben: https://orcid.org/0000-0003-1056-0223

Ana A. Aldana: https://orcid.org/0000-0003-4997-7982

Matthew B. Baker: https://orcid.org/0000-0003-1731-3858

Louis M. Pitet: https://orcid.org/0000-0002-4733-0707

Notes

The authors declare no competing financial interests.

ACKNOWLEDGMENTS

The authors are grateful for partial support (L.M.P., A.A.A., and M.B.B.) from the Research Foundation-Flanders (FWO) under contract G080020N. S.H. is grateful for funding from a BOF-OWB mandate under contract BOF19OWB08. This research has also been made possible with support of NWO (Innovation Fund Chemistry, project "DynAM" under project agreement 731.016.202), and the Dutch Ministry of Economic Affairs.

REFERENCES

1. Lau, H. K.; Kiick, K. L., Opportunities for Multicomponent Hybrid Hydrogels in Biomedical Applications. *Biomacromolecules* **2015,** *16*, 28-42.

2. Lee, J.-H.; Kim, H.-W., Emerging properties of hydrogels in tissue engineering. *J. Tissue Eng.* **2018,** *9*.

3. Wang, Y. N.; Adokoh, C. K.; Narain, R., Recent development and biomedical applications of self-healing hydrogels. *Expert Opin Drug Deliv.* **2018,** *15*, 77-91.

4. Liu, Z.; Xin, W. W.; Ji, J. D.; Xu, J. L.; Zheng, L. J.; Qu, X. H.; Yue, B., 3D-Printed Hydrogels in Orthopedics: Developments, Limitations, and Perspectives. *Front. bioeng. biotechnol.* **2022,** *10*.

5. Kim, I. L.; Mauck, R. L.; Burdick, J. A., Hydrogel design for cartilage tissue engineering: A case study with hyaluronic acid. *Biomaterials* **2011,** *32*, 8771-8782.

6. Fuchs, S.; Shariati, K.; Ma, M., Specialty tough hydrogels and their biomedical applications. *Adv. Healthc. Mater.* **2020,** *9*, 1901396.

7. Gong, J. P.; Katsuyama, Y.; Kurokawa, T.; Osada, Y., Double-network hydrogels with extremely high mechanical strength. *Adv. Mater.* **2003,** *15*, 1155-1158.

8. Aldana, A. A.; Houben, S.; Moroni, L.; Baker, M. B.; Pitet, L. M., Trends in Double Networks as Bioprintable and Injectable Hydrogel Scaffolds for Tissue Regeneration. *ACS Biomater. Sci. Eng.* **2021**.

9. Li, H. J.; Tan, C.; Li, L., Review of 3D printable hydrogels and constructs. *Mater. Des.* **2018,** *159*, 20-38.

10. Hong, S. M.; Sycks, D.; Chan, H. F.; Lin, S. T.; Lopez, G. P.; Guilak, F.; Leong, K. W.; Zhao, X. H., 3D Printing of Highly Stretchable and Tough Hydrogels into Complex, Cellularized Structures. *Adv. Mater.* **2015,** *27*, 4035-4040.

11. He, Y.; Yang, F. F.; Zhao, H. M.; Gao, Q.; Xia, B.; Fu, J. Z., Research on the printability of hydrogels in 3D bioprinting. *Sci. Rep.* **2016,** *6*.

12. Li, J.; Wu, C.; Chu, P. K.; Gelinsky, M., 3D printing of hydrogels: Rational design strategies and emerging biomedical applications. *Mater. Sci. Eng. R Rep.* **2020,** *140*.

13. Advincula, R. C.; Dizon, J. R. C.; Caldona, E. B.; Viers, R. A.; Siacor, F. D. C.; Maalihan, R. D.; Espera, A. H., On the progress of 3D-printed hydrogels for tissue engineering. *MRS Commun.* **2021,** *11*, 539-553.

14. Haas, H. C.; Schuler, N. W., Thermally reversible homopolymer gel systems. *J. Polym. Sci. B* **1964,** *2*, 1095-1096.

15. Dai, X.; Zhang, Y.; Gao, L.; Bai, T.; Wang, W.; Cui, Y.; Liu, W., A Mechanically Strong, Highly Stable, Thermoplastic, and Self-Healable Supramolecular Polymer Hydrogel. *Adv. Mater.* **2015,** *27*, 3566-3571.

16. Li, J.; Yang, J.; Liu, W., A mechanically robust, stiff, and tough hyperbranched supramolecular polymer hydrogel. *Macromol. Rapid Commun.* **2019,** *40*, 1800819.

17. Haas, H. C.; Moreau, R. D.; Schuler, N. W., Synthetic thermally reversible gel systems. II. *J. Polym. Sci., Part A-2: Polym. Chem.* **1967,** *5*, 915-927.

18. Ge, S.; Li, J.; Geng, J.; Liu, S.; Xu, H.; Gu, Z., Adjustable dual temperature-sensitive hydrogel based on a self-assembly cross-linking strategy with highly stretchable and healable properties. *Mater. Horiz.* **2021,** *8*, 1189-1198.

19. Xu, Z.; Liu, W., Poly (N-acryloyl glycinamide): a fascinating polymer that exhibits a range of properties from UCST to high-strength hydrogels. *Chem. Commun.* **2018,** *54*, 10540-10553.

20. Majstorovic, N.; Agarwal, S., Thermosensitive Fluorescence of an UCST-type Hybrid Functional Hydrogel. *ACS Appl. Polym.* **2021,** *3*, 4992-4999.

21. Wu, Q.; Wei, J.; Xu, B.; Liu, X.; Wang, H.; Wang, W.; Wang, Q.; Liu, W., A robust, highly stretchable supramolecular polymer conductive hydrogel with self-healability and thermo-processability. *Sci. Rep.* **2017,** *7*, 41566.

22. Wang, H.; Wu, Y.; Cui, C.; Yang, J.; Liu, W., Antifouling super water absorbent supramolecular polymer hydrogel as an artificial vitreous body. *Adv. Sci.* **2018,** *5*, 1800711.

23. Kuang, L.; Huang, J.; Liu, Y.; Li, X.; Yuan, Y.; Liu, C., Injectable Hydrogel with NIR Light-Responsive, Dual-Mode PTH Release for Osteoregeneration in Osteoporosis. *Adv. Funct. Mater.* **2021,** *31*, 2105383.

24. Xu, Z.; Fan, C.; Zhang, Q.; Liu, Y.; Cui, C.; Liu, B.; Wu, T.; Zhang, X.; Liu, W., A Self-Thickening and Self-Strengthening Strategy for 3D Printing High-Strength and Antiswelling Supramolecular Polymer Hydrogels as Meniscus Substitutes. *Adv. Funct. Mater.* **2021,** *31*, 2100462.

25. Zhai, X.; Ma, Y.; Hou, C.; Gao, F.; Zhang, Y.; Ruan, C.; Pan, H.; Lu, W. W.; Liu, W., 3D-printed high strength bioactive supramolecular polymer/clay nanocomposite hydrogel scaffold for bone regeneration. *ACS Biomater. Sci. Eng.* **2017,** *3*, 1109-1118.

26. Boustta, M.; Colombo, P.-E.; Lenglet, S.; Poujol, S.; Vert, M., Versatile UCST-based thermoresponsive hydrogels for loco-regional sustained drug delivery. *J. Control. Release* **2014,** *174*, 1-6.

27. Wu, Y.; Lu, Y.; Wu, C.; Chen, J.; Ning, N.; Yang, Z.; Guo, Y.; Zhang, J.; Hu, X.; Wang, Y., Conductive dual hydrogen bonding hydrogels for the electrical stimulation of infected chronic wounds. *J. Mater. Chem. B* **2021,** *9*, 8138-8146.

28. Zhang, X.; Yang, X.; Dai, Q.; Zhang, Y.; Pan, H.; Yu, C.; Feng, Q.; Zhu, S.; Dong, H.; Cao, X., Tough thermoplastic hydrogels with re-processability and recyclability for strain sensors. *J. Mater. Chem. B* **2021,** *9*, 176-186.

29. Jin, L.; He, H.; Yang, F.; Xu, L.; Guo, G.; Wang, Y., Tough pNAGA hydrogel hybridized porcine pericardium for the pre-mounted TAVI valve with improved anti-tearing properties and hemocompatibility. *Biomed. Mater.* **2020,** *15*, 065013.

30. Shi, X.; Gao, H.; Dai, F.; Feng, X.; Liu, W., A thermoresponsive supramolecular copolymer hydrogel for the embolization of kidney arteries. *Biomater. Sci.* **2016,** *4*, 1673-1681.

31. Gao, F.; Xu, Z.; Liang, Q.; Liu, B.; Li, H.; Wu, Y.; Zhang, Y.; Lin, Z.; Wu, M.; Ruan, C., Direct 3D printing of high strength biohybrid gradient hydrogel scaffolds for efficient repair of osteochondral defect. *Adv. Funct. Mater.* **2018,** *28*, 1706644.

32. Gao, F.; Xu, Z.; Liang, Q.; Li, H.; Peng, L.; Wu, M.; Zhao, X.; Cui, X.; Ruan, C.; Liu, W., Osteochondral Regeneration with 3D-Printed Biodegradable High-Strength Supramolecular Polymer Reinforced-Gelatin Hydrogel Scaffolds. *Adv. Sci.* **2019,** *6*, 1900867.

33. Zhang, Q.; Xu, Z.; Zhang, X.; Liu, C.; Yang, R.; Sun, Y.; Zhang, Y.; Liu, W., 3D Printed High-Strength Supramolecular Polymer Hydrogel-Cushioned Radially and Circumferentially Oriented Meniscus Substitute. *Adv. Funct. Mater.* **2022**, 2200360.

34. Kim, J.; Zhang, G.; Shi, M.; Suo, Z., Fracture, fatigue, and friction of polymers in which entanglements greatly outnumber cross-links. *Science* **2021,** *374*, 212-216.

35. Zheng, S. Y.; Ding, H.; Qian, J.; Yin, J.; Wu, Z. L.; Song, Y.; Zheng, Q., Metal-Coordination Complexes Mediated Physical Hydrogels with High Toughness, Stick–Slip Tearing Behavior, and Good Processability. *Macromolecules* **2016,** *49*, 9637-9646.

36. Zhang, M.; Ren, X.; Duan, L.; Gao, G., Joint double-network hydrogels with excellent mechanical performance. *Polymer* **2018,** *153*, 607-615.

37. Yang, C. H.; Wang, M. X.; Haider, H.; Yang, J. H.; Sun, J.-Y.; Chen, Y. M.; Zhou, J.; Suo, Z., Strengthening alginate/polyacrylamide hydrogels using various multivalent cations. *ACS Appl. Mater. Interfaced* **2013,** *5*, 10418-10422.

38. Gong, J. P., Why are double network hydrogels so tough? *Soft Matter* **2010,** *6*, 2583-2590.

39. Sun, J. Y.; Zhao, X. H.; Illeperuma, W. R. K.; Chaudhuri, O.; Oh, K. H.; Mooney, D. J.; Vlassak, J. J.; Suo, Z. G., Highly stretchable and tough hydrogels. *Nature* **2012,** *489*, 133-136.

40. Hafeez, S.; Ooi, H. W.; Morgan, F. L. C.; Mota, C.; Dettin, M.; Van Blitterswijk, C.; Moroni, L.; Baker, M. B., Viscoelastic Oxidized Alginates with Reversible Imine Type Crosslinks: Self-Healing, Injectable, and Bioprintable Hydrogels. *Gels* **2018,** *4*.

41. Ooi, H. W.; Mota, C.; ten Cate, A. T.; Calore, A.; Moroni, L.; Baker, M. B., Thiol-Ene Alginate Hydrogels as Versatile Bioinks for Bioprinting. *Biomacromolecules* **2018,** *19*, 3390-3400.

42. Aldana, A. A.; Morgan, F. L. C.; Houben, S.; Pitet, L. M.; Moroni, L.; Baker, M. B., Biomimetic double network hydrogels: Combining dynamic and static crosslinks to enable biofabrication and control cell-matrix interactions. *J. Polym. Sci.* **2021,** *59*, 2832-2843.

43. Smeets, K.; Slane, J.; Scheys, L.; Claes, S.; Bellemans, J., Mechanical analysis of extra-articular knee ligaments. Part one: native knee ligaments. *The Knee* **2017,** *24*, 949-956.

44. Rongen, J. J.; van Tienen, T. G.; van Bochove, B.; Grijpma, D. W.; Buma, P., Biomaterials in search of a meniscus substitute. *Biomaterials* **2014,** *35*, 3527-3540.

45. Shepherd, D. E.; Seedhom, B. B., The'instantaneous' compressive modulus of human articular cartilage in joints of the lower limb. *Rheumatology* **1999,** *38*, 124-132.

46. Means, A. K.; Grunlan, M. A., Modern strategies to achieve tissue-mimetic, mechanically robust hydrogels. ACS Macro Letters, 2019.

47. Wiegand, C.; Hipler, U. C., Evaluation of biocompatibility and cytotoxicity using keratinocyte and fibroblast cultures. *Skin Pharmacol. Physiol.* **2009,** *22*, 74-82.

48. Davidson, S.; Coles, M.; Thomas, T.; Kollias, G.; Ludewig, B.; Turley, S.; Brenner, M.; Buckley, C. D., Fibroblasts as immune regulators in infection, inflammation and cancer. *Nat. Rev. Immunol.* **2021,** *21*, 704-717.

Graphic for Table of Contents